Supporting Information

Controlled the Intermolecular Proton Coupled Electron Transfer Process: A Novel Design Strategy for the Highly Sensitive Piezo-chromic Fluorescent Materials

Miao Yu,†[a] Jingping He,†[a] Zhenzhen Xu,*[a] Zhongwei Man,[b] Ping Wang,[a] Yuhao Xiang,[a] Fei Yu [a] and Hongbing Fu *[a]

† Miao Yu and Jingping He contributed equally.

Miao Yu, Jingping He, Zhenzhen Xu, Ping Wang, Yuhao Xiang, Fei Yu, Hongbing Fu

Beijing Key Laboratory for Optical Materials and Photonic Devices,

Department of Chemistry, Capital Normal University,

Beijing 100048, P. R. China.

E-mail: hbfu@cnu.edu.cn; xuzhenzhen@cnu.edu.cn.

Zhongwei Man

School of Chemical Engineering and Technology,

Institute of Molecular Plus, Tianjin University,

Tianjin 300072, China.

General Methods

Characterization Techniques: The compound was confirmed by High resolution mass spectroscopy (ESI-MS), ^{1}H NMR (600 MHz, DMSO-d_6, 293K) and^{13}C NMR (400 MHz, DMSO-d_6, 293K).

Spectral measurement: The steady-state absorption spectra were measured on a Shimidazu UV-3600 spectrophotometer. The diffuse reflectance absorption spectra were measured on a Hitachi UH-5700 UV-VIS-NIR spectrophotometer. The emission spectra were measured on Horiba FluoroMax-4-NIR spectrophotometers.

Time-resolved Fluorescence spectra. The fluorescence lifetime and time-resolved emission spectrum detected with a streak camera (C10647, Hamamatsu Photonics) upon 400 nm femtosecond laser excitation.

Fluorescence quantum yield. The relative fluorescence quantum yields of solutions were measured by relative method (using Rhodamine B as a reference (Φ_f = 0.70 in basic ethanol) and absolute method (using the integrating sphere equipped on FluoroMax-4-NIR spectrophotometer), respectively. To avoid the internal filter effect, the absorbance of the solutions was maintained below 0.1.

The pressure value applied on the sample: The exact pressure value applied on the sample was determined by the formula "Pressure= Force / Force area". The "Force Area" were the area of all the crystals on the glass substrate. And the "Force" was forming pressure indicator on the digital thrust gauge.

Preparation of the crystals. Two kinds of polymorph crystals with high quality and homogeneity were obtained in high throughput under difference growth conditions. G-type single crystals were prepared by slowly evaporating of the 5 mL saturated dichloromethane solution in the 10 mL glass sample at room temperature. B-type single crystals were prepared by diffusing *n*-hexane vapor into TPAC dichloromethane solution at room temperature.

Theoretical calculations. Geometrical and electronic structures of all states were calculated by Gaussian 16 program package. The geometric structure of ground state (S_n) in solid was optimized by density functional theory（DFT）and time-dependent density functional theory（TDDFT）combined with the quantum mechanics/molecular mechanics（QM/MM）model. Given the weak interactions between molecules，the dimer was based on the TDDFT-D3 calculation. Based on the optimized molecular structure at S_0, the excitation energies of the n-th singlet state (S_n) and the n-th triplet state (T_n) were calculated by TD-DFT method. The oscillator strength (*f*) was performed using the B3LYP function and the 6-31g (d) basis set at the best geometry of the lowest single excited state (S_1).

Syntheses and Structural Characterization

Commercially available reagents and solvents were used without further purification unless otherwise noted. Compound TPAC was synthesized to the procedure described in Scheme S1. 4-Diphenylaminobenzaldehyde, acetone and potassium permanganate are purchased from Innochem.
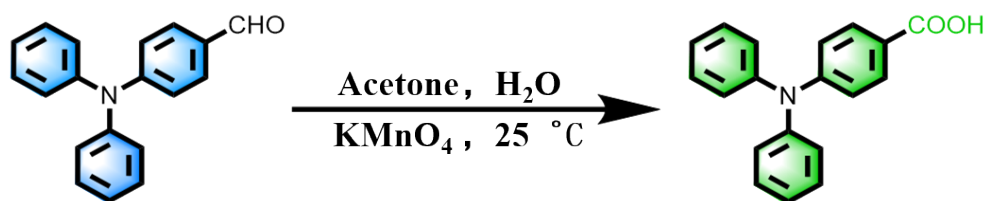
Scheme S1. Synthetic routes to compound TPAC.

3g of 4-diphenylaminobenzaldehyde was dissolved in a mixture of 50 mL of acetone and water (volume ratio 4.5:1), 4.3 g of potassium permanganate was slowly added, and the mixture was stirred and refluxed at room temperature for 8 h. After the reaction is cooled to room temperature, the solvent is dried and distilled water is added to it for filtration; After adding a few drops of dilute hydrochloric acid, a white flocculent precipitate was generated, filtered, and dried to obtain powder (yield 54.2%).
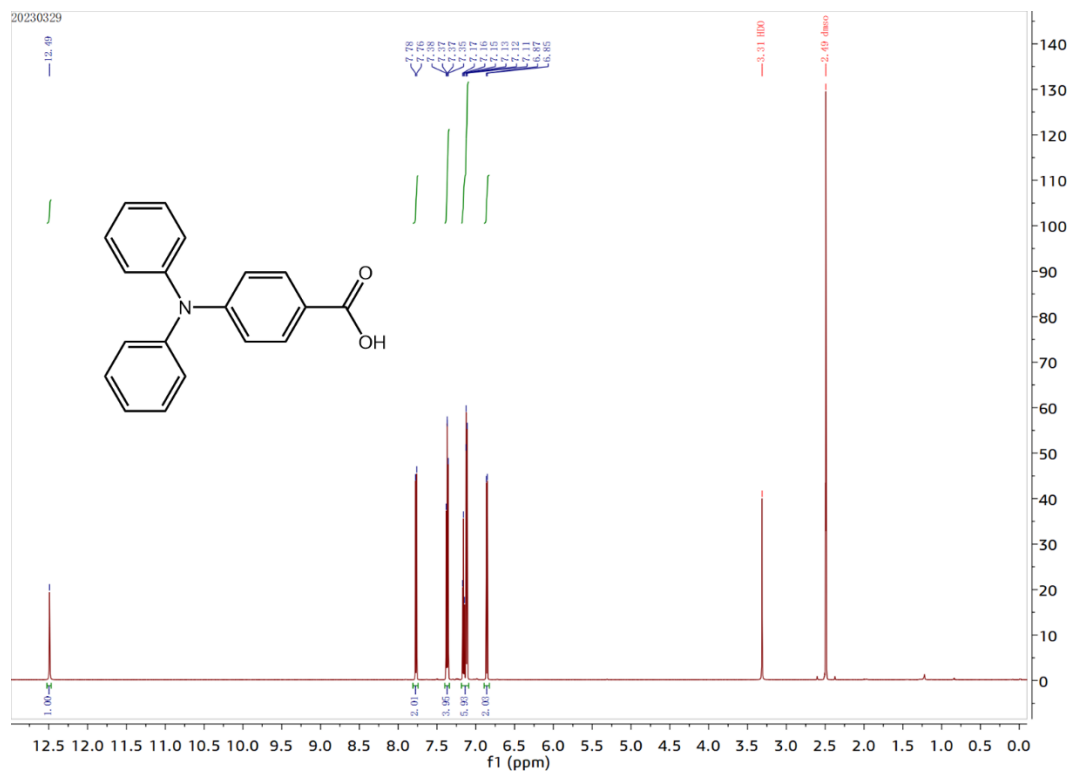
Figure S1. ^{1}H NMR spectrum of compound TPAC. ^{1}H NMR (600 MHz, DMSO-d_6 δ): 12.48 (s, 1H), 7.78 – 7.73 (m, 2H), 7.39 – 7.32 (m, 4H), 7.14 (tt, J = 7.5, 1.2 Hz, 2H), 7.13 – 7.07 (m, 4H), 6.87 – 6.82 (m, 2H).
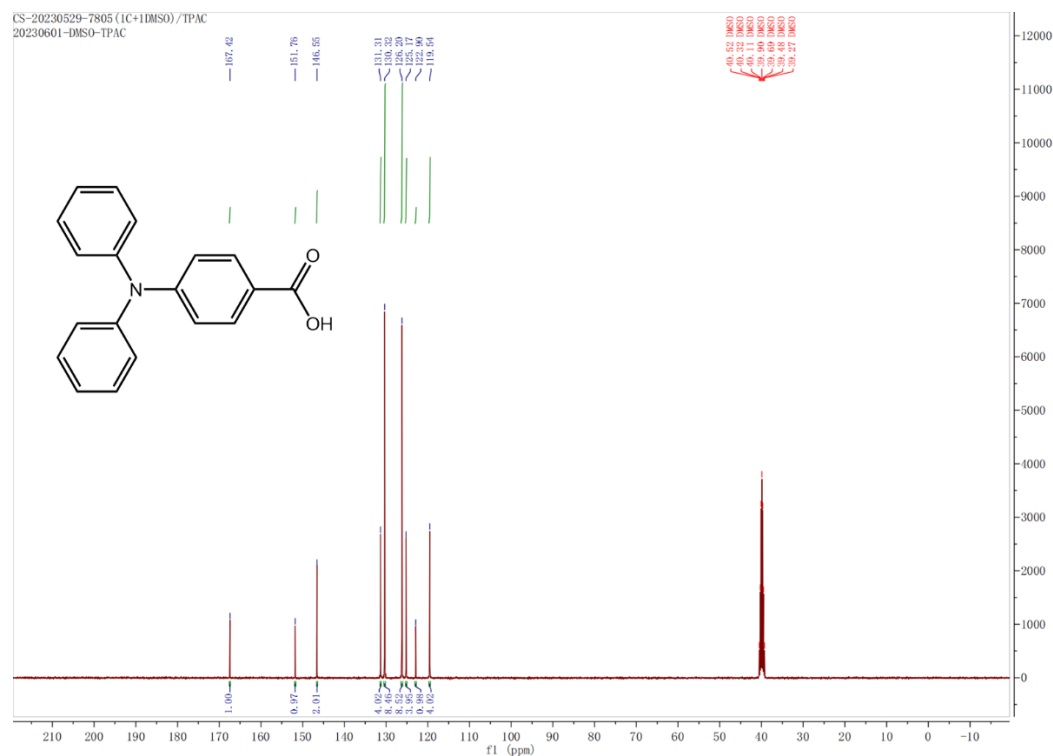
Figure S2. ^{13}C NMR spectrum of compound TPAC. ^{13}C NMR (101 MHz, DMSO-d_6) δ = 167.42, 151.76, 146.55, 131.31, 130.32, 126.20, 125.17, 122.90, 119.54.
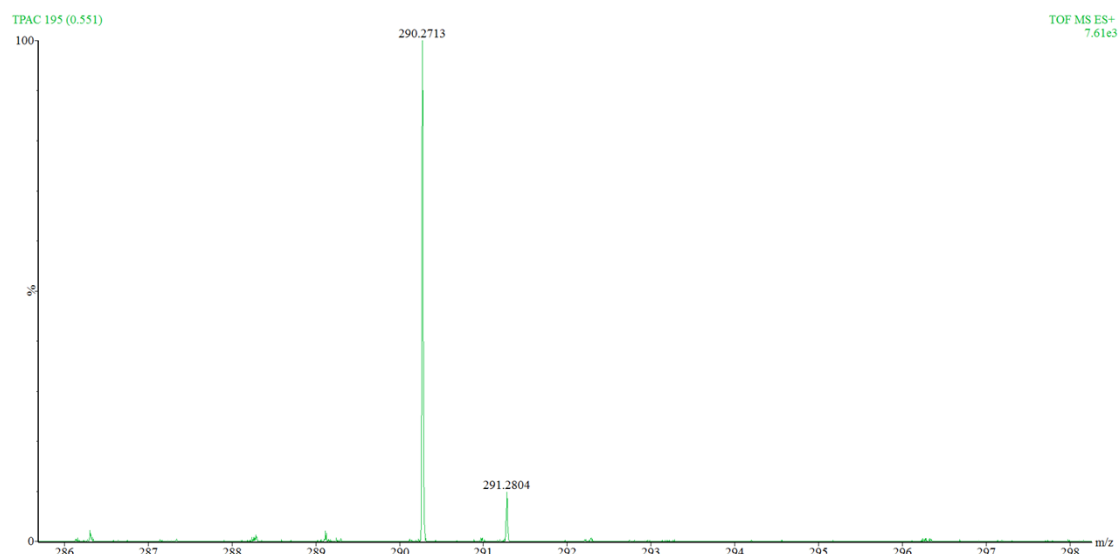
Figure S3. HRMS (ESI): *m/z* [M + H] $^{+}$ calcd for $C_{19}H_{15}NO_2$, 289.11; found, 290.2713.
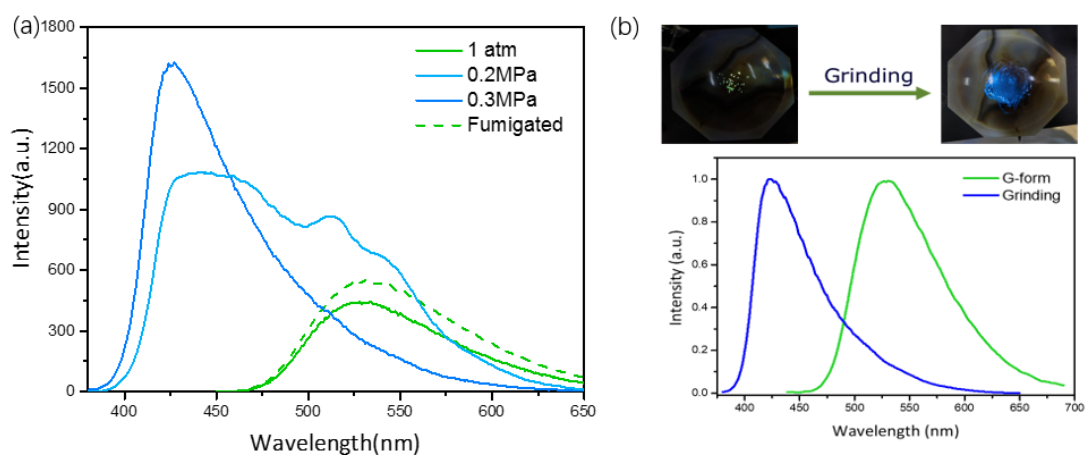
Figure S4. (a) Emission spectra of G-type crystals after being pressed at different pressure and after fumigation with DCM vapor. **(b)** The Photograph and emission spectra from a ground powder of G-type crystal under UV irradiation at 365 nm.

- Clearly, spectrum of the powders with cyan emission (0.2 Mpa) is a combination of spectrum of G-type crystals and spectrum of e powders with blue emission (0.3 Mpa).
- In order to investigate the response of TPAC G-type crystals to anisotropic forces, mechanical grinding with a mortar and pestle was performed. The test results show that the uniaxial pressure also could change emission color from green to blue with an enhanced emission.

Table S1. Summary of the single crystals data of G-form and B-form.

	TPAC-G	TPAC-B
CCDC	2222048	2222049
Crystal system	monoclinic	monoclinic
Space group	$P2_1/n$	$P2_1/n$
a/Å	9.2349(6)	9.3100(10)
b/Å	9.6558(8)	9.7399(8)
c/Å	17.2969(13)	17.6380(17)
α/°	90	90.00
β/°	90.280(7)	90.742(9)
γ/°	90	90.00
Volume/Å^3	1542.4(2)	1599.2(3)
Z	4	4
ρ_{calc}g/cm^3	1.246	1.202
Goodness-of-fit on F2	1.041	0.862
Final R indexes [I >= 2σ (I)]	R1 = 0.0416, wR2 = 0.0929	R_1 = 0.0643, wR_2 = 0.1411
Final R indexes [all data]	R1 = 0.0555, wR2 = 0.1019	R_1 = 0.0804, wR_2 = 0.1760
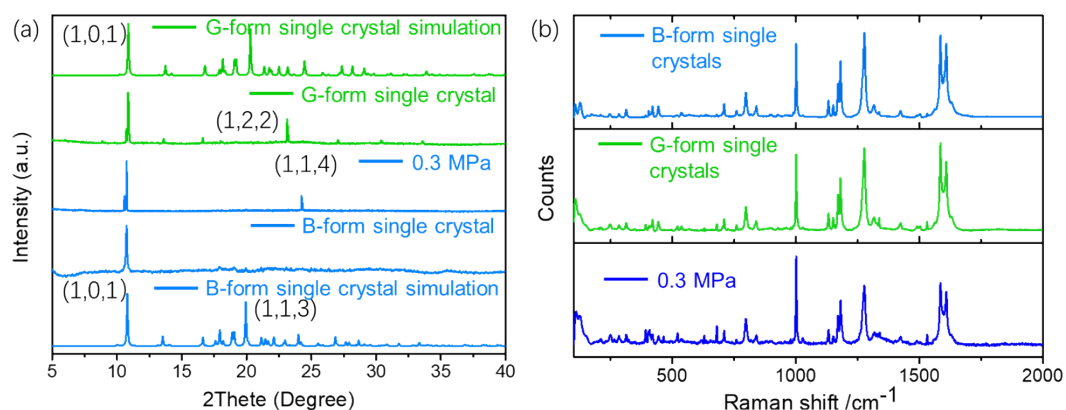
Figure S5. XRD patterns (a) and Raman spectra (b)of G-type and B-type crystals and pressed (0.3 MPa) G-type crystals. For comparison, the simulated powder XRD spectrum (bottom) using Mecury software is also included in (a).

● The simulated PXRD results of the G-and B-type single crystals data as shown in Figure

S5 are almost the same, indicating the same molecular packing. The PXRD analysis of the G-type crystal, B-type crystal, and the pressed G-type crystalline powder at 0.3 MPa were also performed and well matched with the simulated pattern. The slight peaks shift, the differences in intensity and the missing of the partial diffraction peaks in the experimental data as compared to the simulated pattern can be ascribed to the great difference of experiment temperature and the preferred orientation in the crystals with size of mm.

- The Raman spectra of G-type single crystals, B-type single crystals and and the pressed G-type crystalline powder (0.3 MPa) were almost the same, indicating the similar molecular packing structure, which is consistent with the single crystal data.
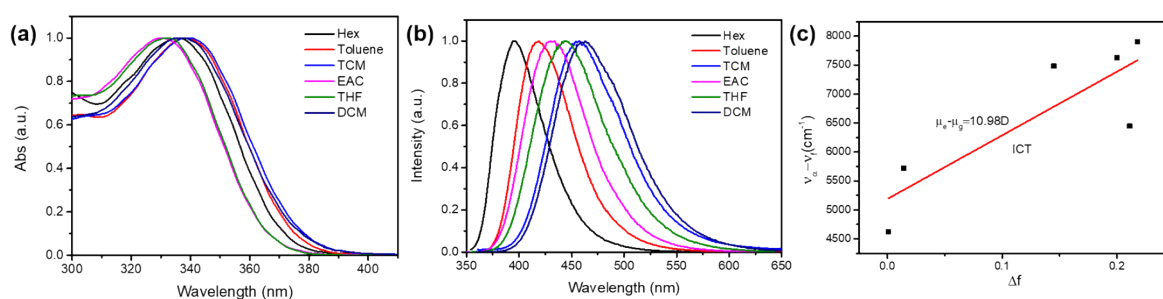
Figure S6. The photophysical properties of TPAC in different solvents. a) Normalized absorption spectra of TPAC in different solutions. b) The emission spectra of TPAC in different solutions. c) Linear correlation of the orientation polarization ($\triangle$f) of the solvent media with the Stokes shift (v_a-v_f) for TPAC.

Table S2. Photophysical data of TPAC in different solvents.

	λ_{abs} (nm)	λ_{em} (nm)	Stokes' shift (nm)	ε (L mol^{-1} cm^{-1})	$\triangle$f
Hexane	334	395	61	30814	0.001
Toluene	338	419	81	28871	0.014
TCM	340	456	116	28800	0.145
EtAC	330	431	101	31814	0.200
THF	333	424	91	29512	0.211
DCM	339	463	124	29056	0.218

HOMO   LUMO
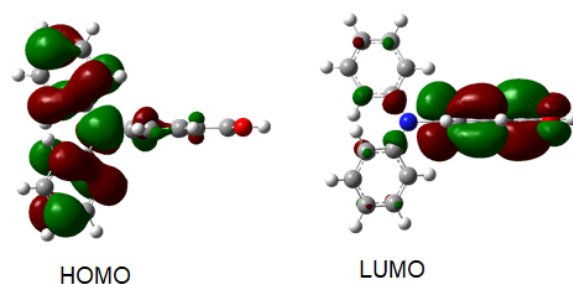
Figure S7. The energy level of TPAC molecules in crystal G-form single crystal and B-form single crystal is calculated.

➤ As typical D-A compounds, TPAC displayed CT features. The absorption and emission spectra of TPAC in different solvents were studied and the results were shown in Figure S6 and Table S2.

➤ With increasing polarity of the solvent from non-polar n-hexane to highly polar DCM solution, the absorption maxima of TPAC molecules varied slightly between 330 and 340 nm, while the emission maximum shifted from 395 to 463 nm, exhibiting remarkable solvato-fluorochromic behavior. According to the Lippert−Mataga equation, the $\mu_e-\mu_g$ was calculated to be 10.98 D, ascribed to a CT state.[1]

➤ Figure S7 presents the natural transition orbitals of TPACs at their single-crystal configurations. The electron clouds of the highest occupied molecular orbital (HOMO) are delocalized over the entire backbone, while the LUMO level is mainly located on the benzene ring attached to the carboxylic acid, together revealing an CT feature.
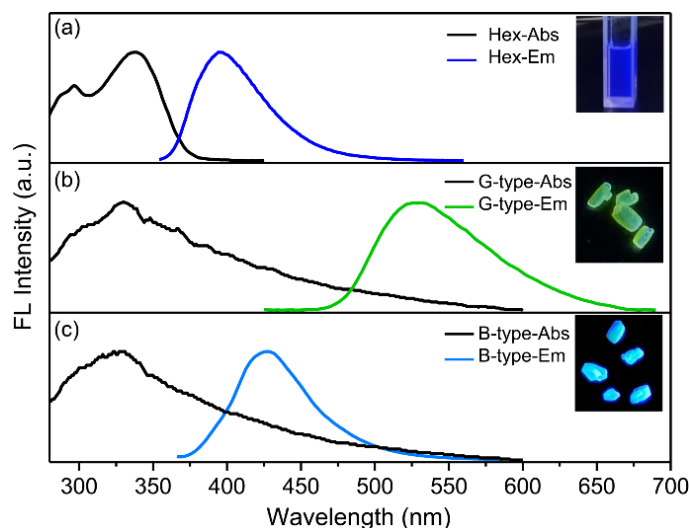
Figure S8. Normalized absorption and emission spectra of TPAC in n-hexane solution (a), G-type single crystals (b) and B-type single crystals (c). The insets are the corresponding fluorescent images under UV light (365 nm).
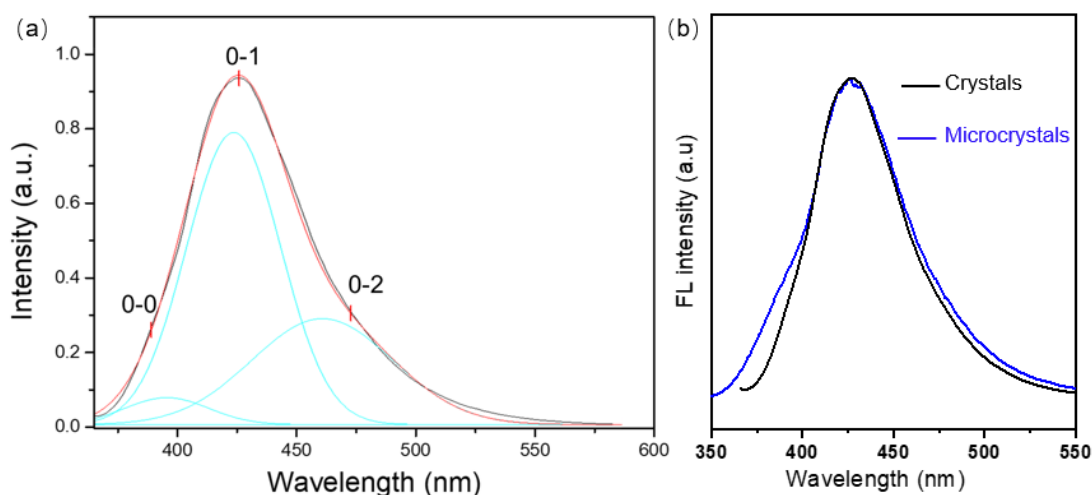
Figure S9. (a) Peak fitting spectra of emission spectra of B-type crystals. (b) The emission spectra of B-type crystals (black lines) and microcrystals (blue lines).

- The emission spectra of B-form exhibits a vibronic progression, with 0-0 transition at 395.2 nm (25303 cm^{-1}), 0-1 transition at 424.6 nm (23551 cm^{-1}) and 0-2 transition at 459.6 nm (21758 cm^{-1}) as shown in Figure S9a, with a subband spacing of 1750–1800 cm^{-1}, arising mainly from C=O stretching vibration modes.
- To further demonstrate this point, the B-type microcrystals were prepared through a simple reprecipitation method. As shown in Figure S9b, the maximum of the emission peak was consisted with the B-Type crystals. Moreover, the 0-0 transition at 395 nm was more pronounced, possibly due to reduced self-absorption effect in microcrystals.
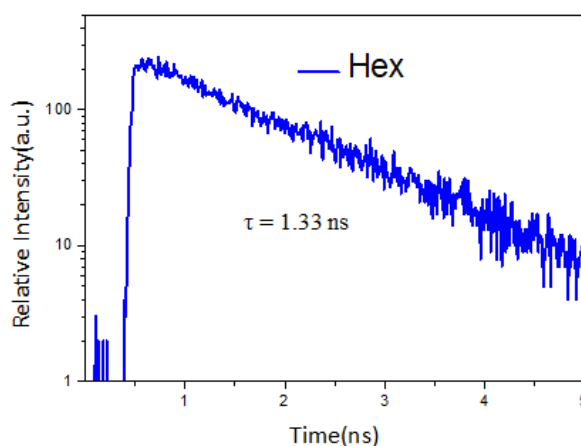
Figure S10. Fluorescence decay profiles of the TPAC monomers in Hex solution.

(b)
*Baeline x(1)= 1.1335
*Amplitude-I x(2)= -59.8984
*Amplitude-II x(6)= 128.3866
*Rate-I x(3)= 2.9746 1/ps
*Rate-II x(7)= 0.54086 1/ps
*Time Origin x(4)= 0.3929 ps
*HWHM of IRF x(5)= 0.043474 ps
LIFETIMES:
*lifetime-1= 0.33618 ps+/-0.14767ps
*lifetime-2= 1.8489 ps+/-0.15462ps
Chi^2=:
     5.0229

?[2 82.01 5.33 0.35 0.1 90.26 0.37]
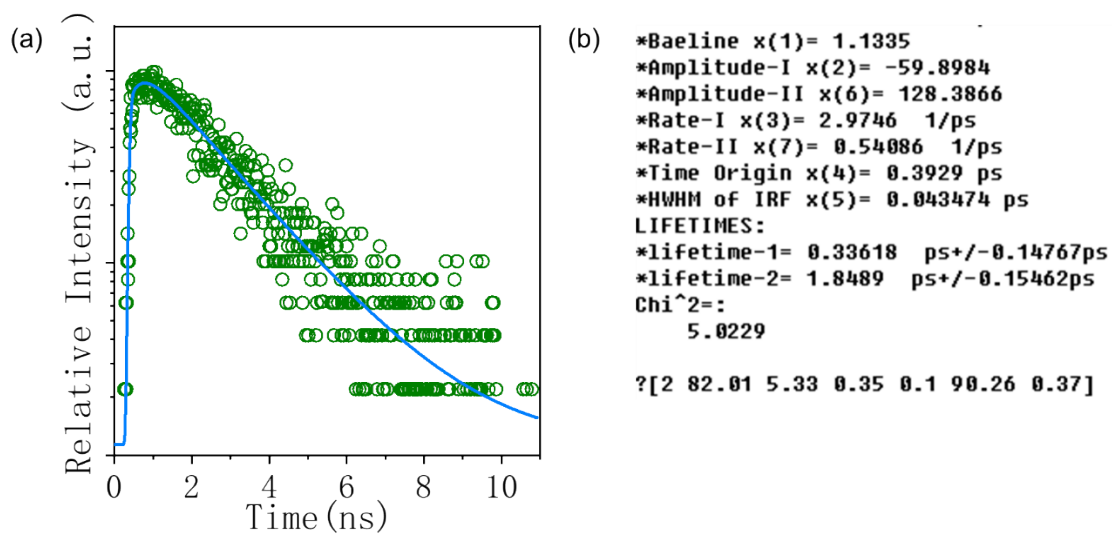
Figure S11. The decay curve of G-type crystals at 530 nm.
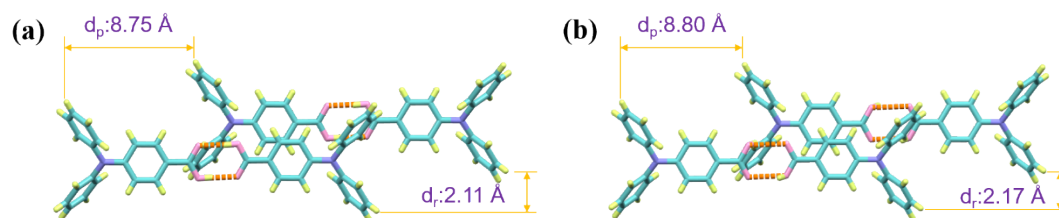
Figure S12. The slip distance of the dimers of G-form single crystal (a) and B-form single crystal (b) along the major (d_p) and minor axes (d_r).
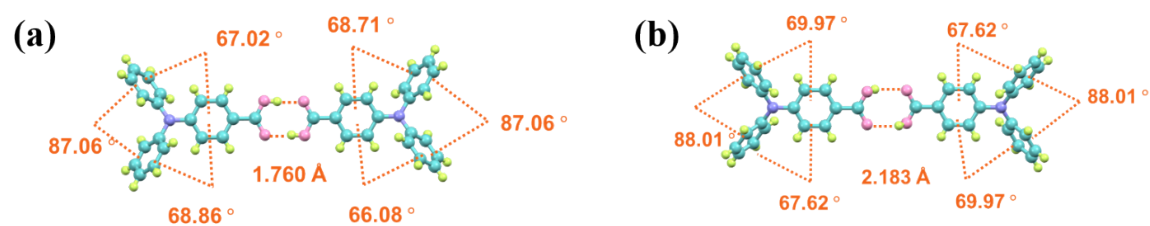
Figure S13. G-form single crystal (a) and B-form single crystal (b) adjacent benzene ring dihedral angle.
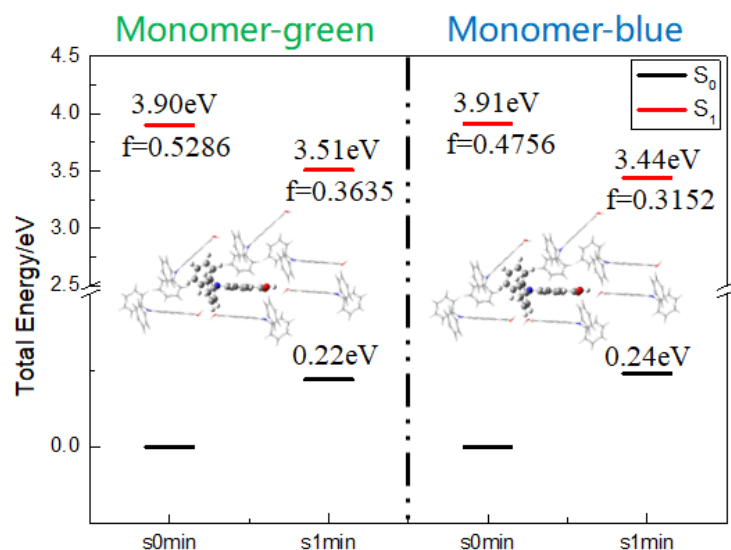
Figure S14. Calculate the energy level of TPAC molecular monomers in crystal G-type and B-type single crystal.

- The calculation results show that the energy difference caused by molecular conformations is 0.09 eV.
- Considering that the emission spectra is blue-shifted by 105 nm form G-type to B-type, the molecular conformational alteration from G-type single crystal to B-type single crystal is not the main reason for their differences in emission spectra.
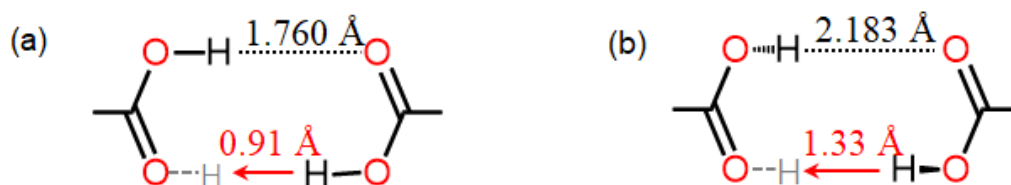
Figure S15. Top view of the intermolecular hydrogen bond of G-type single crystals (a) and B-type single crystals (b).
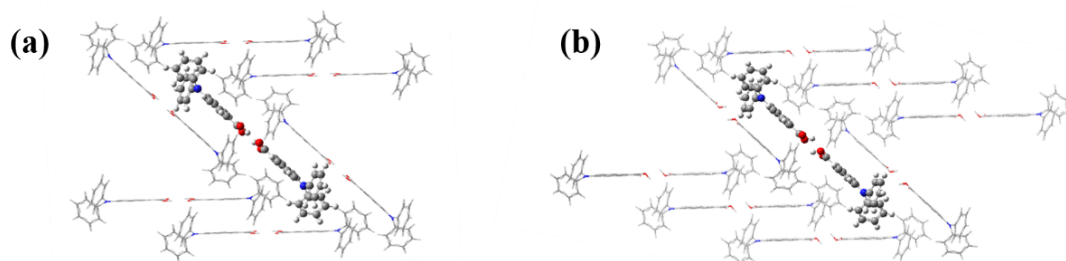
Figure S16. Quantum/molecular mechanics (QM/MM) calculations by embedding a dimer of TPAC (QM part at B3LYP-D3/6-31g(d) level) into its crystal lattice. (a) G-type crystal. (b) B-type crystal.
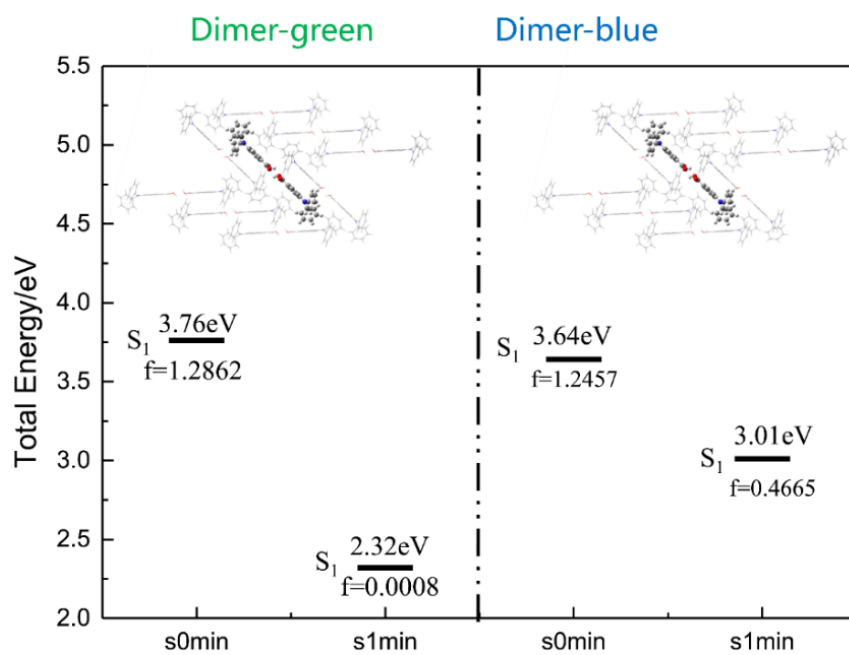
Figure S17. Calculate the energy level of TPAC molecular dimers in crystal G-type single crystal and B-type single crystal.
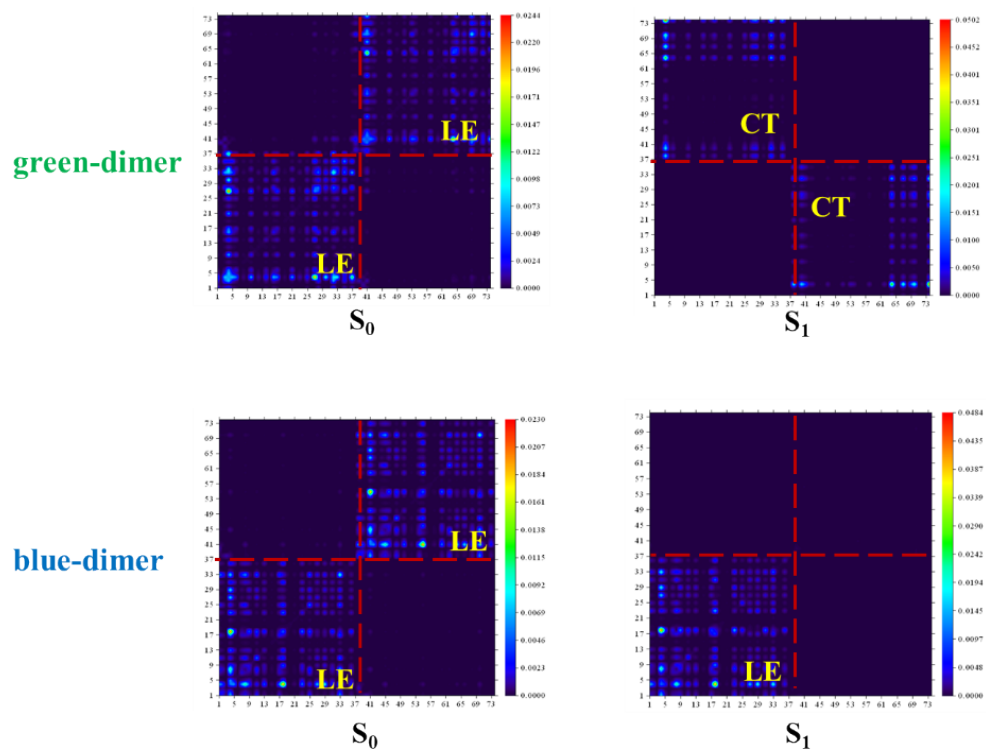
Figure S18. The TDM map of a TPAC dimers.
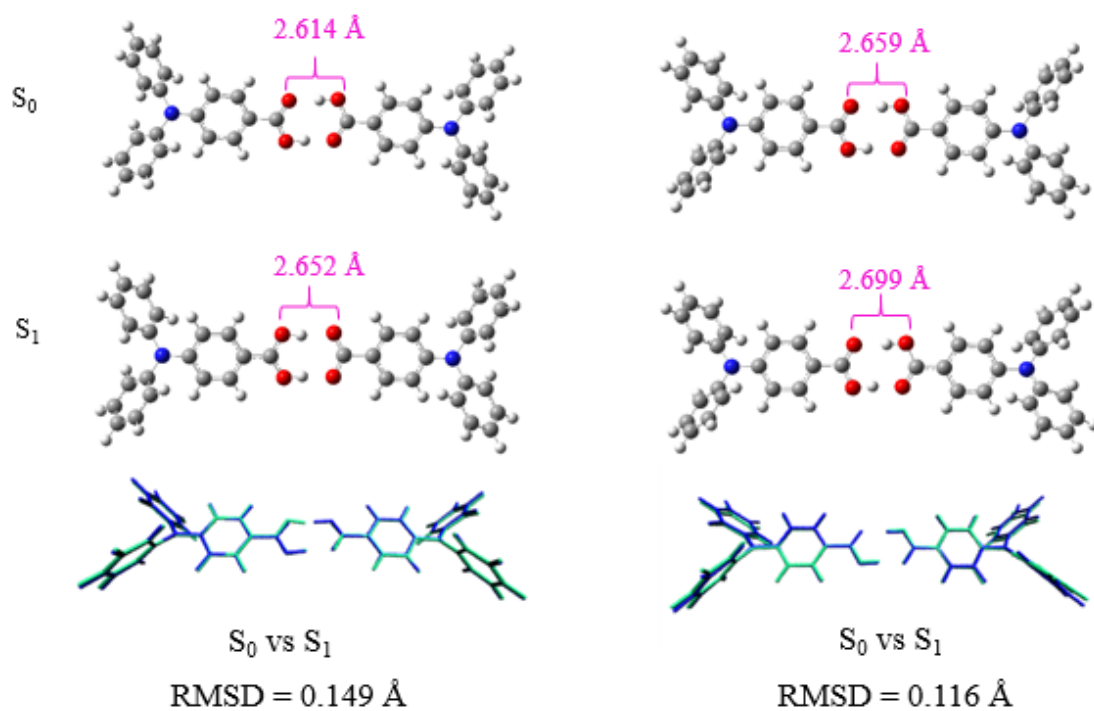
Figure S19. The optimized S_0 and S_1 configurations and visible geometry changes between S_0 and S_1 of G-type (left) and B-type (right) crystals.
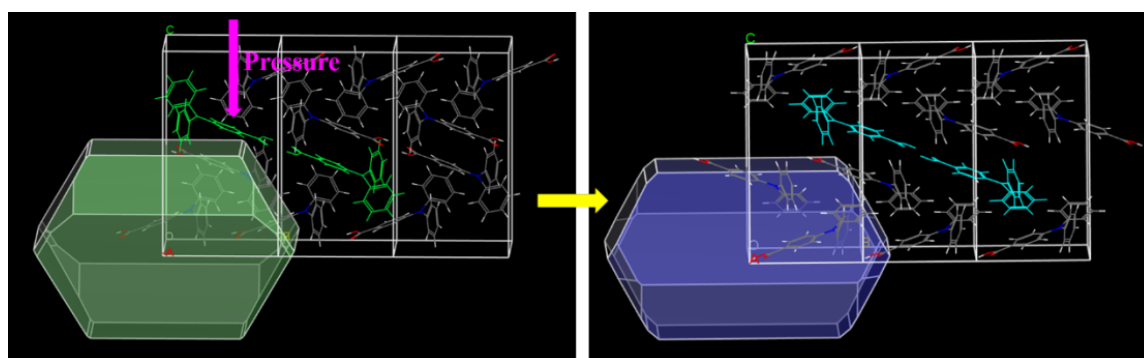
Figure S20. Equilibrium shape of G-type (left) and b) B-type single crystal for minimum total surface energy, calculated by the Materials Studio package software.
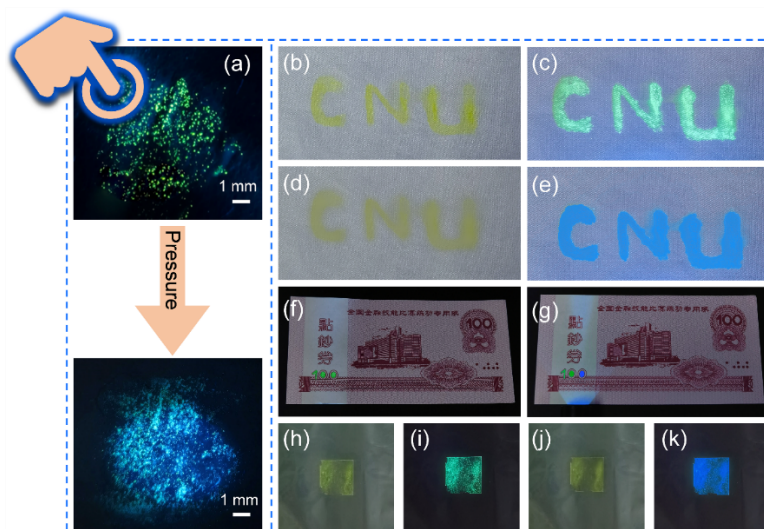
Figure S21. (a) Film image of TPAC ink droplets formed on filter paper, above: before pressing, below: after pressing. (b-e) Images of the word "CNU" written used the ink on the fabric: under daylight (b, d) and UV lamp of 365nm (c, e); before pressing (b, c) and after pressing (d-e). Images printed as an anti-counterfeiting ink on a 100 RMB practice note (not a genuine note) with the number "100" under an ultraviolet lamp: (f) an unpressed pattern, and (g) the number "100" is partially pressed. (h-k) Images of ink droplets formed on plastic: under daylight (h, j) and UV lamp (i, k); before pressing (h, i) and after pressing (j, k).

- Encouraged by the highly sensitive PCF properties with high emission, the G-form TPAC microcrystals aqueous inks were prepared. The preparation procedure is as follows: after the prepared poly (vinyl alcohol) PVA aqueous solution (0.05 $g \cdot mL^{-1}$) was prepared via dissolving 1 g of PVA in 20 mL of DI water at 80 °C for 2 h. Disperse 10 mg TPAC microcrystals with sizes of about 200 μm into 1 mL of the above PVA aqueous solution. which was then stirred for 10 min to form a homogeneous TPAC ink. Drop TPAC ink onto the filter paper to form a uniform film, and gently press with your fingers to change from a more luminous green color to a stronger blue color.

- Note that the TPAC microcrystals encapsulated in the PVA medium still maintain the sensitive PCF behaviors after completely drying in air. Drop TPAC ink onto the filter paper to form a uniform film, and gently press with your fingers to change from a more luminous green color to a stronger blue color. More impressively, TPAC ink can be drawn on different flexible substrates, including glass, fabric, plastic, paper, and so on, which shows great potential applications in the field of haptic sensors and wearable flexible anticounterfeiting devices.

References

[1] J. A. Mondal, H. N. Ghosh, T. K. Ghanty, T. Mukherjee, D. K. Palit, *J. Phys. Chem. A* **2006**, *110*, 3432-3446.